

Electronic structure and bond competition in the polar magnet PbVO_3

D. J. Singh

Condensed Matter Sciences Division, Oak Ridge National Laboratory, Oak Ridge, TN 37831-6032, USA

Density functional electronic structure studies of tetragonal PbVO_3 are reported. The results show an important role for both Pb 6p-O 2p and V d-O p bonding, with an interplay between these. This is discussed in relation to the possibility of obtaining magnetoelectric behavior.

I. INTRODUCTION

Magnetoelectric and specially multiferroic magnetoelectrics have attracted renewed attention,^{1,2,3,4} although the field has a long history.^{5,6,7,8,9} Nonetheless, bulk materials that provide strong coupling between electric and magnetic fields at room temperature remain elusive. Some of the difficulties in realizing such materials were reviewed by Hill.³ Perovskite and perovskite-derived phases, ABO_3 , provide the main inorganic ferroelectric materials used in applications. These are based on a cubic lattice with A ions on the cube corners and B ions at the cube centers, inside corner sharing octahedral O cages. Ferroelectric perovskites can be classified as A-site or B-site driven according to which ion is primarily responsible for the polar instability. One strategy for synthesizing multiferroics is to substitute one of the perovskite sites with magnetic ions in materials where the ferroelectricity is driven by the other site, as for example in BiFeO_3 .¹⁰ However, in both A and B-site driven materials the ferroelectricity generally involves cooperation between off-centerings of both cations, and furthermore covalency between unoccupied metal states and O p states is important for the ferroelectric instability.^{11,12,13,14,15,16} From this point of view, V^{4+} may be a particularly interesting ion for multiferroics.

In oxides, V^{4+} is often magnetic and, significantly, can occur either at the centers of octahedral cages, as in CaVO_3 and SrVO_3 , in which case there are interesting metal-insulator transitions of Mott character,^{17,18} or it can strongly bind to one O forming forming a vanadyl ion with very short bond length, $1.55-1.60$ Å. These vanadyl-containing compounds are local moment magnets due to the formation of spin 1/2 moments on the V ions, and are band insulators. The band gaps are formed by a combination of strong crystal field splitting associated with the short V-O distance, and on-site Hund's coupling, which exchange splits the 1/2 filled V non-bonding orbital.^{19,20} Thus, perovskite vanadates offer the possibility of combining a magnetic B-site ion with insulating behavior and stereochemical activity on both the A and B-sites. This was recently realized by the high pressure synthesis of PbVO_3 .^{21,22}

PbVO_3 is insulating and occurs in the tetragonal, non-centrosymmetric structure, spacegroup $\text{P}4=\text{mm}$, like PbTiO_3 , but with a very large tetragonality, $c/a=1.23$. The structural distortion may be described as off-centering of Pb and V accompanied by a distortion of the

VO_6 octahedral cage. This is in contrast to CaVO_3 and SrVO_3 , which have centrosymmetric GdFeO_3 type structures deriving from octahedral tilting. PbVO_3 shows no structural transitions from 0K to the decomposition temperature. However, a tetragonal to cubic transition does occur under pressure,²² indicating the possibility of ferroelectric behavior under pressure and perhaps by chemical modification. It is noteworthy that at 300K the shortest V-O distance is 1.67 Å, which is longer than in most other vanadyl-containing oxides. This implies that the vanadyl bond is relatively weak in PbVO_3 . Furthermore, because of the connection between the short V-O bond and the moment formation, one may anticipate the possibility of coupling between magnetism and the structural distortion, which in turn, if ferroelectric, would be coupled to external electric field. Significantly, the Pb displacement with respect to the center of its O cage is 0.92 Å, and the V displacement is 0.60 Å. These are large and of comparable magnitude, indicating both robust ferroelectricity if switching could be achieved, and cooperativity between the two cation sites, which is a characteristic of good ferroelectric perovskites.

Shpanchenko and co-workers²¹ reported local spin density approximation (LSDA) electronic structure calculations and an analysis of the bonding and magnetism. These calculations were based on the linearized muffin-tin orbital method with the atomic spheres approximation (LMTO-ASA). This method is well suited to magnetic transition metal oxides, but is suffers from shape and basis set errors in open structures with highly non-cubic site symmetries, as is the case for PbVO_3 . They also reported LSDA+U calculations for ferromagnetic ordering only, with the augmented plane wave plus local orbital (APW+LO) method. The comparison of these two leads to the conclusion that the formation of the spin polarized vanadyl bond depends on Hubbard correlation effects. Here we report LDA calculations done with the general potential linearized augmented plane wave (LAPW) method, which incorporates the full crystal potential and has a much better basis set than the LMTO-ASA method, especially for the interstitial regions.²³ We use these to discuss the formation of the electronic structure and the bonding of the compound. We find results that differ significantly from those of Ref. 21, with a different conclusion regarding the vanadyl bond. Our results compare well with very recent calculations of Uratani and co-workers.²⁴ We find an interplay between Pb-O and V-O covalency that may be of importance for magnetoelectric materials.

II. COMPUTATIONAL METHOD

As mentioned, the calculations were done using the general potential LAPW method. Except as noted, the experimental 300K crystal structure reported by Belik and co-workers²² was used. The calculated LSDA forces on the atoms are small with this structure, supporting the experimental determination as well as the conclusion that the vanadyl bond is properly formed at the LSDA level. The largest force is on the apical O of 0.032 Ry/ a_0 towards the V, with a smaller force of 0.017 Ry/ a_0 drawing the V towards the apical O for the lowest energy (see below) antiferromagnetic ordering. The LAPW sphere radii were 2.00 a_0 , 1.70 a_0 , and 1.35 a_0 , respectively for Pb, V and O. Local orbitals²⁵ were used to treat the high lying valence states of Pb and V, as well as to relax linearization errors. The basis sets consisted of approximately 1100 LAPW functions plus local orbitals for the primitive cells and correspondingly larger sizes for supercells. Zone sampling during the iterations to self-consistency was done using the special points method, with 40 k-points in the irreducible wedge for the primitive cell. Tests with other choices were made. These showed that the calculations were well converged. Magnetic ordering was studied using $2 \times 2 \times 2$ supercells. In all cases, the core states were treated self-consistently and fully relativistically, while the valence states were calculated in a scalar relativistic approximation.

III. MOMENT FORMATION

Stable spin moments of 1 μ_B were found for all magnetic configurations, consistent with local moment magnetism. This differs from the calculations reported in Ref. 21, where the F ordering showed only a small moment in contrast to the C ordering. As mentioned, they also did LSDA + U calculations for the ferromagnetic case, but with the APW + LO method instead of the LMTO-ASA method that they used for the other calculations in their paper. The implication of their results is that the Hubbard U is essential for a stable spin polarized vanadyl bond. We find a stable spin polarized bond in accurate LSDA calculations, with the implication that the key physics is hybridization with O and on-site Hund's coupling. Calculations were done for an artificial non-spin-polarized case, as well as ferromagnetic (F), antiferromagnetic in the ab plane (C), antiferromagnetic along all three directions (G), and ferromagnetic ab planes stacked antiferromagnetically along the c-direction (A). The calculated energies are given in Table I.

We find the lowest energy state to be antiferromagnetic type C, qualitatively in agreement with the calculations of Ref. 21, and with energies in good agreement with those of Ref. 24. We note that the energies are not well described by a nearest neighbor Heisenberg model. Both the C and G orderings have antiferromagnetic ab planes but opposite stacking along c. Similarly, F and

TABLE I: Energetics of various spin configurations of PbVO_3 relative to the non-spin-polarized case. Energies are given in meV per formula unit.

| F | G | A | C |
|--------|--------|-------|--------|
| -111.2 | -127.3 | -91.8 | -127.8 |

A have ferromagnetic ab planes, again differing in the c stacking. However, the energies of C and G differ by less than 1 meV per V, while those of F and A differ by approximately 19 meV. Thus interactions at least to second neighbor are needed to reconcile the energies. Considering this, as well as the extremely small energy difference between the C and G orderings, the actual ground state could be complex. One may speculate that this is the reason for non-observation of antiferromagnetic superlattice peaks in neutron diffraction. We note that there is evidence for a transition at 120K seen both in thermal expansion²² and resistivity.²¹

IV. BAND STRUCTURE

We now turn to the electronic structure, starting with the F ordering. The band structure is shown in Fig. 1, and the corresponding density of states (DOS) and projections in Fig. 2. The band structure, in order of increasing energy, consists of a split-off Pb 6s derived peak, approximately 9 eV below the Fermi energy followed by a manifold of O 2p derived bands, and then, following another gap, a manifold of metal derived bands. Initially, these are V d derived, but at higher energy (~ 3 eV) these change to include Pb p and other characters.

The crystal field may be regarded as a combination of an octahedral crystal field, which splits the d levels into a lower lying t_{2g} group and a higher lying e_g group. These are then further split by the octahedral centering. The main contribution to the crystal field in oxides is from metal-oxygen hybridization. Since the O 2p bands are below the V d bands, the V d orbitals are formally antibonding, so the stronger the hybridization of a given d orbital with O, the higher it will be pushed. The result is a splitting of the e_g manifold into two and a splitting of the t_{2g} manifold into a low lying d_{xy} non-bonding band and a higher two-fold degenerate d_{xz} and d_{yz} derived manifold. This explains the multipipe structure of the d band DOS. In the case of V^{4+} , there is one d electron in the d_{xy} orbital, which forms local moments due to the Hund's coupling. The exchange splitting for F ordering is 1.43 eV, and not sensitive to the magnetic ordering (see Fig. 3). This is sufficient to fully polarize the d orbitals. For F ordering this yields a half-metallic state, spin moment 1 μ_B .

With the experimental structure of PbVO_3 and F ordering, the crystal field splitting is almost, but not quite, sufficient to open a complete gap between the majority

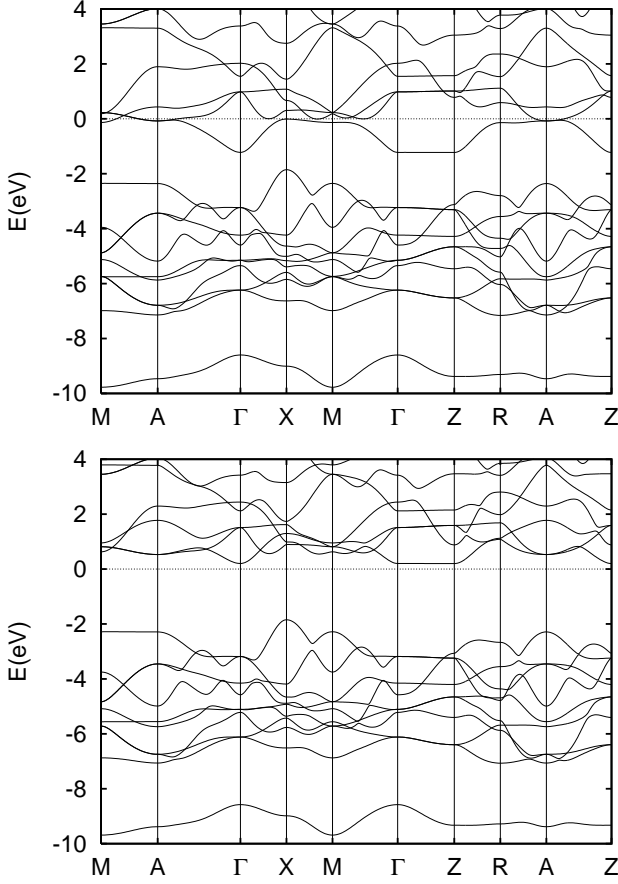


FIG. 1: Band structure of ferromagnetic ordered PbVO_3 . The top panel shows the majority spin bands and the bottom shows the minority spin.

spin d_{xy} band and the higher lying d bands. This is because of the bandwidth of the d_{xy} band. As may be seen in majority spin panel of Fig. 1, the d_{xy} band has almost no dispersion along the Z line and has weak dispersion along M-A implying that the main hopping is the ab plane. Following the dispersion along M, the d_{xy} band maximum is 0.3 eV above the bottom of the other d bands.

We did a structural relaxation for the F ordering. The resulting LSDA positional parameters are $z_V = 0.5689$, $z_{O1} = 0.2158$, and $z_{O2} = 0.6872$, yielding a V-O1 bond length of 1.67 Å, which is slightly less than the experimental value. The corresponding experimental values are $z_V = 0.5668$, $z_{O1} = 0.2102$, and $z_{O2} = 0.6889$. The calculated full symmetry a_g Raman frequencies are 190 cm^{-1} (Pb motion against the other atoms in the cell), 408 cm^{-1} (cations vs. O), and 838 cm^{-1} (V-O1 bond stretching, reflecting the short bond length and steric interaction).

The effect of in-plane antiferromagnetism is to narrow the d_{xy} band by disrupting nearest neighbor hopping. This is because the exchange splitting is large. The result is a band gap as shown in Fig. 3. Because the crystal field splitting is sensitive to the exact V-apical O distance,

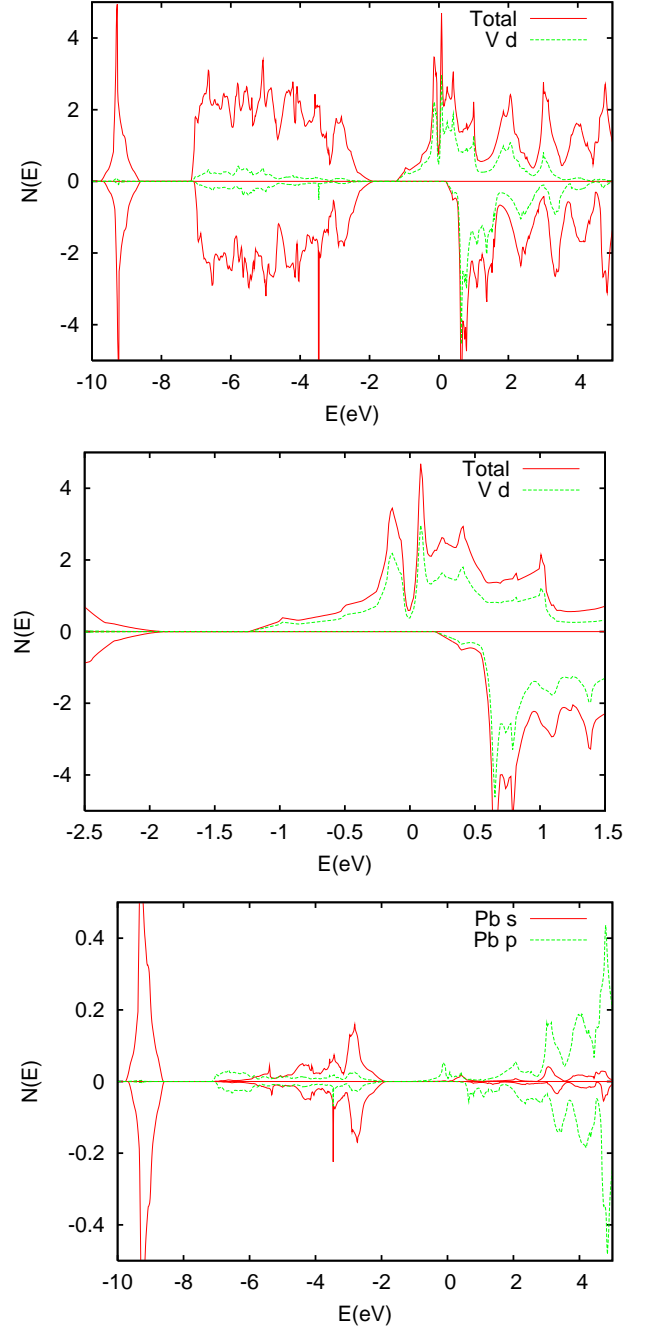


FIG. 2: (color online) Electronic DOS and projections onto LAPW spheres for ferromagnetic PbVO_3 . The top panel shows the total DOS and projections onto the V d character, while the bottom shows Pb contributions. The middle panel is a blow up around E_F . Note that since the Pb orbitals are more extended than the $2a_0$ sphere radii, the Pb projection is proportional to the corresponding contributions, but reduced in magnitude. Majority and minority spin are shown above and below the axes, respectively.

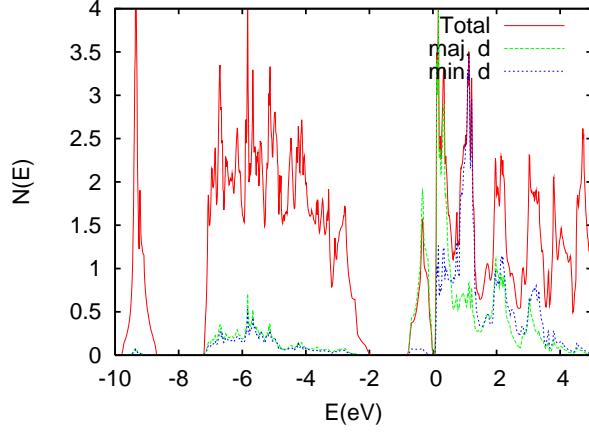


FIG. 3: (color online) Electronic DOS of PbVO_3 for the lowest energy C-type antiferromagnetic ordering.

the band gap should also be sensitive to this structural parameter. We can also understand in these terms why the energy difference between the G and C type orderings is small and that between the F and A type orderings is not, even though both pairs differ only in the c direction magnetic stacking. Specifically, in the F and A orderings, the majority d_{xy} manifold overlaps the other d states so that the moment is not of pure d_{xy} character, and there are non-trivial dispersions in the c direction in the region of the zone where there is overlap, such as M-A of Fig. 1. These dispersions provide interaction along c, and because they consist of ismetallic d band overlap in only one spin channel, the resulting spin interaction is strongly ferromagnetic. Thus F is strongly favored over A. On the other hand, with antiferromagnetic in-plane ordering, the d bands are narrower, and so the d_{xy} band does not overlap the other d states. Thus the c axis exchange coupling is much weaker. At the experimental structure it is very weakly ferromagnetic, favoring C over G, but if the gap were larger, either due to a shortening of the V-apical O distance or on-site Coulomb repulsions, one would expect it to become antiferromagnetic. In this case, if the magnetic structure is simple, the ground state would become G type. Thus, at least at the LSDA level, PbVO_3 is near a structure dependent cross-over between two magnetic states.

V. ROLE OF Pb

Turning now to the role of Pb, the bottom panel of Fig. 2 shows projections of the DOS onto the Pb LAPW sphere (radius $2a_0$). The large peak below the O 2p bands is from the Pb 6s states. As may be seen, these mix with the occupied O 2p bands, but play almost no role in the unoccupied conduction bands. Mixing of occupied states does not produce bonding. On the other hand, the Pb 6p states are low lying in the conduction bands and

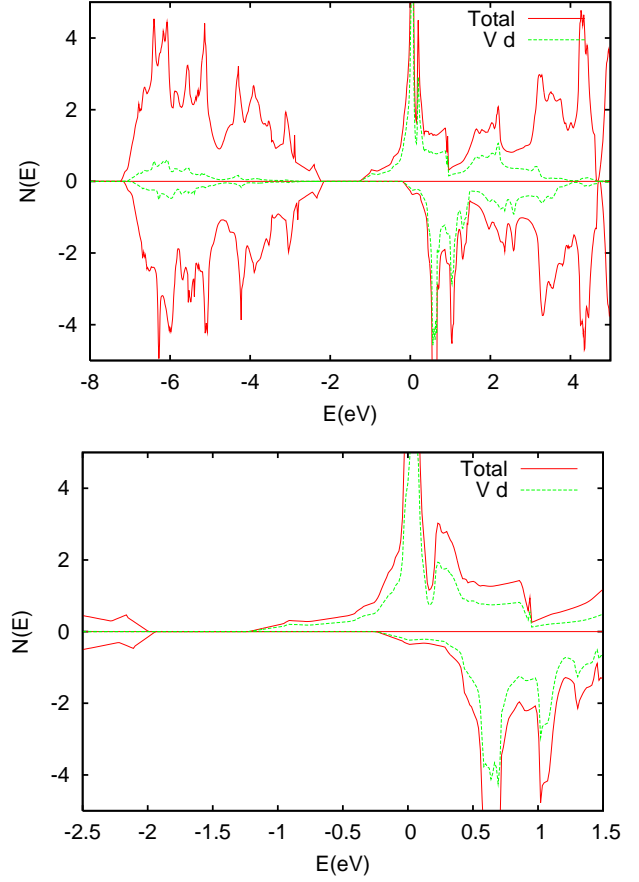


FIG. 4: (color online) Electronic DOS of hypothetical ferromagnetic CaVO_3 constrained to the PbVO_3 crystal structure (see text) and a blow-up around E_F .

mix with the O 2p bands, which are the same bands that hybridize with V d states. Thus there is a mechanism for competition between the vanadyl bonding and the Pb-O bonding.

We emphasize that while the lone 6s pair of Pb^{2+} is often discussed in terms of the stereochemical activity of Pb, these orbitals are not responsible for the activity directly. Rather it is that in Tl(I), Pb(II) and Bi(III) the atomic structure that leads to the position of the 6s orbital also leads to 6p levels that are low lying in the conduction bands and very spatially extended favoring hybridization with occupied ligand orbitals. We emphasize that while the lone 6s pair of Pb^{2+} is often discussed in terms of the stereochemical activity of Pb, these orbitals are not responsible for this activity directly. Rather it is that in Pb(II) and Bi(III) the atomic structure that leads to the position of the 6s orbital also leads to 6p levels that are low lying in the conduction bands and very spatially extended favoring hybridization with occupied ligand orbitals.

Sr^{2+} is similar in size to Pb^{2+} , but does not have the lone pair and the resulting low lying spatially extended

unoccupied p states. As a result, it would not form structures with short bond lengths to O like the reported structure of PbVO_3 . Ca^{2+} is a smaller ion, also lacking the lone pair, and is more compatible with the bond lengths in PbVO_3 , though, as mentioned, CaVO_3 actually forms a centrosymmetric tilted GdFeO_3 type structure. As such, we did calculations for hypothetical ferromagnetic ordered CaVO_3 with the atomic positions fixed at those of PbVO_3 in order to elucidate the role of Pb. The calculated DOS is shown in Fig. 4. As may be seen, the pseudogap between the majority spin d_{xy} band and the remaining d bands is reduced and the half-metallic character is lost (the spin moment is $0.88 \mu_B$ instead of $1 \mu_B$). As mentioned, in PbVO_3 the calculated forces on the atoms are small. Keeping the structure fixed, there is a strong force of $0.08 \text{ Ry}/a_0$ pushing the V away from the apical O, i.e. disrupting the vanadyl bond. Thus indeed there is substantial coupling between the Pb-O interaction and the V-O interaction, seen both in the stability of the vanadyl bond and the magnetic properties. This is due to bond competition with O. Specifically, the removal of Pb leads to broadening of the t_{2g} bands, which which spoils the crystal field scheme that stabilizes the

vanadyl bond.

VI. SUMMARY

To summarize, LSDA calculations support the experimental conjecture that PbVO_3 may be the basis for interesting magnetoelectric materials. This is based on the electronic coupling between Pb and V due to mutual bonding with O and the stabilization of magnetism by a mechanism connected with the V-O bonding. The key challenge is to find chemical modifications that make the material more switchable, so that ferroelectricity can be observed.

Acknowledgments

We are grateful for helpful discussions with Y. Shimakawa. This work was supported by the U.S. Department of Energy and the Office of Naval Research.

-
- ¹ N.A. Spaldin and M. Fiebig, *Science* 309, 391 (2005).
 - ² M. Fiebig, Th. Lottermoser, D. Frohlich, A.V. Goltssev, and R.V. Pisarev, *Nature (London)* 419, 818 (2002).
 - ³ N.A. Hill, *J. Phys. Chem. B* 104, 6694 (2000).
 - ⁴ T. Kimura, T. Goto, H. Shintani, K. Ishizaka, T. Arima, and Y. Tokura, *Nature (London)* 426, 58 (2003).
 - ⁵ P. Curie, *J. Phys. (Paris) Ser. III* 3, 393 (1894).
 - ⁶ G.A. Smolenskii and I. Chupis, *Sov. Phys. Usp.* 25, 475 (1982).
 - ⁷ G.A. Smolenskii, A.I. Granovskaya, S.N. Popov, and V.A. Isupov, *Sov. Phys. Tech. Phys.* 3, 1981 (1958).
 - ⁸ G.A. Smolenskii, V.A. Isupov, and A.I. Granovskaya, *Sov. Phys. Solid State* 1, 150 (1959).
 - ⁹ G.A. Smolenskii, A.I. Granovskaya, and V.A. Isupov, *Sov. Phys. Solid State* 1, 907 (1959).
 - ¹⁰ J.W. ang, J.B. Neaton, H. Zheng, V. Nagarajan, S.B. Ogale, B. Liu, D. Viehland, V. Vaithyanathan, D.G. Schlom, U.V. Waghmare, N.A. Spaldin, K.M. Rabe, M. Wuttig, and R. Ramesh, *Science* 299, 1719 (2003).
 - ¹¹ R.E. Cohen and H. Krakauer, *Phys. Rev. B* 42, 6416 (1990).
 - ¹² R.E. Cohen, *Nature (London)* 358, 137 (1992).
 - ¹³ D.J. Singh and L.L. Boyer, *Ferroelectrics* 136, 95 (1992).
 - ¹⁴ D.J. Singh, *Phys. Rev. B* 53, 176 (1996).
 - ¹⁵ I. Grinberg, V.R. Cooper, and A.M. Rappe, *Nature (London)* 419, 909 (2002).
 - ¹⁶ M. Ghita, M. Fomari, D.J. Singh, and S.V. Halilov, *Phys. Rev. B* 72, 054114 (2005).
 - ¹⁷ A. Fujimori, I. Hase, H. Namatame, Y. Fujishima, Y. Tokura, H. Eisaki, S. Uchida, K. Takegahara, and F.M.F. de Groot, *Phys. Rev. Lett.* 69, 1796 (1992).
 - ¹⁸ I.H. Inoue, C. Bergemann, I. Hase, and S.R. Julian, *Phys. Rev. Lett.* 88, 236403 (2002).
 - ¹⁹ W.E. Pickett, *Phys. Rev. Lett.* 79, 1746 (1997).
 - ²⁰ R.C. Rai, J. Cao, J.L. Musfeldt, D.J. Singh, X. Wei, R. Jin, Z.X. Zhou, B.C. Sales, and D.G. Mandrus, *Phys. Rev. B* (submitted).
 - ²¹ R.V. Shpanchenko, V.V. Chemaya, A.A. Tsvirin, P.V. Chizhov, D.E. Sklovsky, E.V. Antipov, E.P. Khlybov, V. Pomjakushin, A.M. Balagurov, J.E. Medvedeva, E.E. Kaul, and C. Geibel, *Chem. Mater.* 16, 3267 (2004).
 - ²² A.A. Belik, M. Azuma, T. Saito, Y. Shimakawa, and M. Takano, *Chem. Mater.* 17, 269 (2005).
 - ²³ D.J. Singh, *Planewaves Pseudopotentials and the LAPW Method* (Kluwer Academic, Boston, 1994).
 - ²⁴ Y. Uratani, T. Shishidou, F. Ishi, and T. Oguchi, *Japanese J. Appl. Phys.* 44, 7130 (2005).
 - ²⁵ D. Singh, *Phys. Rev. B* 43, 6388 (1991).